

Estimating the baryon fraction in the IGM from well-localized FRBs and DESI data

Thais Lemos,^{a,1}

^aObservatório Nacional, Rio de Janeiro - RJ, 20921-400, Brazil

E-mail: thaislemos@on.br

Abstract. Current measurements of Baryon Acoustic Oscillations (BAO) from the Dark Energy Spectroscopic Survey (DESI DR2), when combined with data from Type Ia supernovae (SNe), challenge the observational viability of the Λ -Cold Dark Matter (Λ CDM) model, motivating combinations of independent datasets to estimate cosmological quantities. In a previous communication, we presented a cosmological independent method to constrain the baryon fraction in the IGM (f_{IGM}), where we derived relevant expressions for the dispersion measure (DM) in terms of luminosity distance, allowing us to estimate f_{IGM} combining directly measurements of 17 well-localized FRBs and 1048 SNe from the Pantheon catalog. Here we revisit this method to constrain f_{IGM} , considering two parameterizations for the f_{IGM} : constant and time-dependent. We expand our sample by combining 107 well-localized Fast Radio Bursts (FRBs) with BAO measurements from DESI DR2 and SNe observations from DESY5, and the Pantheon+ catalog. We find through a Bayesian model selection analysis that a conclusive answer about the evolution of f_{IGM} cannot be achieved from the current FRBs observational data. In particular, our results show weak evidence in favor of the constant case.

¹Corresponding author

Contents

1	Introduction	1
2	FRB's theory	2
3	Data and Methodology	3
3.1	Data	3
3.1.1	FRBs	3
3.1.2	BAO	4
3.1.3	SNe Ia	4
3.2	Methodology	5
4	Results	5
5	Conclusions and discussions	8

1 Introduction

The Baryon Acoustic Oscillations (BAO) measurements from the Dark Energy Spectroscopic Instrument (DESI) [1], combined with data from the cosmic microwave background (CMB) and Type Ia supernovae (SNe), provide important results that challenge the Λ CDM paradigm. More precisely, the DESI collaboration reported strong evidence for an evolving dark energy component showing tighter constraints on the dark energy equation of state (EoS) using different $w(a)$ parameterizations [2–4]. In addition to the discrepancy with Λ CDM, DESI Data Release 2 (DESI DR2) [5] provides the most precise and up-to-date BAO data set. In this context, this discrepancy in the current cosmological paradigm motivates the combination of independent cosmological datasets as well as the use of cosmological model-independent approaches as a precise and accurate method to constrain the fundamental cosmological parameters.

We combine DESI measurements with fast radio burst (FRB) data to constrain cosmological/astrophysical parameters. The FRBs are radio transient events with millisecond durations and an unknown origin (for a review, see [6–10]). However, the large observed dispersion measure (DM) comparable to the Milky Way contribution suggests a cosmological origin for these events [12]. Although ~ 1000 FRBs have been detected since the discovery in 2007 by the Parkes telescope [11], only a few of them in the literature are well localized (with redshift). The DM combined with the redshift of the host galaxy can be used as an astrophysical and cosmological probe (see [13–19] for applications of FRBs in the cosmology). In practice, some issues hinder the application of FRBs for cosmological purposes. For instance, the poor knowledge about the dispersion measure's variance related to the spatial variation in the cosmic electron distribution. To circumvent this problem, such fluctuations (δ) can be parameterized as a function of redshift [20]. Another restriction is the variation with respect to the redshift of the fraction of baryon mass in the intergalactic medium (IGM), called as f_{IGM} , which is degenerated with the cosmological parameters. In [21], the authors found $f_{\text{IGM}} \approx 0.82$ at $z \geq 0.4$, while in [22] the authors estimated $f_{\text{IGM}} \approx 0.9$ at $z \geq 1.5$.

In a previous communication [18], we proposed a cosmology-independent method that combines directly the dispersion measure of 17 FRB observations and the luminosity distance (D_L) from supernovae type Ia (SNe) measurements of the Pantheon catalog to constrain a possible evolution of the baryon fraction in the IGM. In the present paper, we revise such method extending our dataset to study the impact of different D_L measurements in this type of analysis, combining 107 well-localized FRBs with BAO measurements from DESI DR2 [5], and with SNe catalogs from Pantheon+ [71], and Dark Energy Survey Supernova 5-Year (DES Y5) [72]. We organized this paper as follows. In Section 2 we briefly present the FRB’s concepts. The datasets used and our model-independent method are presented in Section 3. In Section 4, we present our main results. Finally, we summarize the main conclusions in Sec. 5.

2 FRB’s theory

The FRB’s photons interact with the free electrons in the medium along the path from the source to the observer on Earth. These interactions lead to a change in the frequency of the photons, causing a delay in their arrival time. This time delay is related to the DM, for which the observed dispersion measure can be expressed in terms of other components [23, 24]

$$\text{DM}_{\text{obs}} = \sum_i \text{DM}_i(z), \quad (2.1)$$

where the index $i = \text{ISM, halo, IGM, and host}$ represents the Milky Way interstellar medium (ISM), the Milky Way halo, the intergalactic medium, and host galaxy contributions, respectively.

The quantity $\text{DM}_{\text{obs}}(z)$ of a FRB is directly measured from the corresponding event, while $\text{DM}_{\text{MW,ISM}}$ can be well-determined using models of the ISM galactic electron distribution in the Milky Way from pulsar observations [25–27]. Moreover, the Milky Way halo contribution is not entirely understood yet, and we assume $\text{DM}_{\text{halo}} = 50 \text{ pc}/\text{cm}^3$ [28].

The host galaxy contribution is not a well-understood parameter due to the challenges in measurement and modeling, because it depends on the type of galaxy, the relative orientations of the FRB source with respect to the host and source, and the near-source plasma [29]. For this reason, we consider

$$\text{DM}_{\text{host}}(z) = \frac{\text{DM}_{\text{host},0}}{1+z}, \quad (2.2)$$

where the term $(1+z)$ accounts for the cosmic dilation [23, 30] and $\text{DM}_{\text{host},0}$ is the host galaxy contribution in the source frame and will be a free parameter in our analysis.

The last and largest contribution of the dispersion measure is the IGM, where the cosmological contribution appears. The average of IGM dispersion measure can be written as [23]

$$\text{DM}_{\text{IGM}}(z) = \frac{3c\Omega_b H_0^2}{8\pi G m_p} \int_0^z \frac{(1+z') f_{\text{IGM}}(z') \chi(z')}{H(z')} dz', \quad (2.3)$$

where c , Ω_b , H_0 , G , m_p , $f_{\text{IGM}}(z)$, $H(z)$ are the speed of light, the present-day baryon density parameter, the Hubble constant, the gravitational constant, the proton mass, the baryon fraction in the IGM and the Hubble parameter at redshift z , respectively. While $\chi(z) = Y_H \chi_{e,H}(z) + Y_{He} \chi_{e,He}(z)$ is the free electron number fraction per baryon, in which $Y_H = 3/4$

and $Y_{He} = 1/4$ are the mass fractions of hydrogen and helium, respectively, and $\chi_{e,H}(z)$ and $\chi_{e,He}(z)$ are the ionization fractions of hydrogen and helium, respectively. The hydrogen and helium are fully ionized at $z < 3$ [22, 31], so that we have $\chi_{e,H}(z) = \chi_{e,He}(z) = 1$.

From Eq. 2.1, we can define the observed extragalactic dispersion measure to perform a statistical comparison between the observational data and the theoretical parameters:

$$DM_{\text{ext}}^{\text{obs}}(z) \equiv DM_{\text{obs}}(z) - DM_{\text{ISM}} - DM_{\text{halo}} , \quad (2.4)$$

and the theoretical extragalactic dispersion measure

$$DM_{\text{ext}}^{\text{th}}(z) \equiv DM_{\text{host}}(z) + DM_{\text{IGM}}(z) . \quad (2.5)$$

3 Data and Methodology

3.1 Data

In what follows, we will describe the observational datasets for dispersion measure and luminosity distance that we use in this work.

3.1.1 FRBs

The currently available sample of FRBs contains 116 well-localized events (for details of FRBs catalog ¹, see [32]). We exclude from our analysis the following events: FRB 20171020A [33], FRB 20181030 [34] and FRB [35] have a low redshift ($z = 0.0087$, $z = 0.0039$ and $z = 0.023686$, respectively) and can not be associated with any SNe Ia in the DES catalog; FRB 20190520B [36] has a host galaxy contribution significantly larger than the other events; FRB 20190614 [37] has no measurement of spectroscopic redshift and can be associated with two host galaxies; FRB 20200120E [38] is estimated in direction of M81, but a Milky Way halo can not be rejected; and finally, FRB 20210405I [39] and FRB 20220319D [40] have the MW contribution larger than observed one.

We list in Table 3 our working sample that contains 107 FRBs [35, 40, 42–68] with their main properties: redshift, the Milky Way galaxy contribution ($DM_{\text{MW,ISM}}$) estimated from the NE2001 model [26], observed dispersion measure (DM_{obs}), DM_{obs} uncertainty (σ_{obs}) and the references. For the 41 FRBs marked with the symbol † in σ_{obs} , the uncertainty in DM_{obs} is not provided. In these cases, the uncertainty is randomly drawn from a Gaussian distribution constructed using the mean and standard deviation of the σ_{obs} values from the other events.

The observational quantity DM_{ext} (Eq. 2.4) can be calculated from Table 3 and its total uncertainty can be expressed by the relation

$$\sigma_{\text{tot}}^2 = \sigma_{\text{obs}}^2 + \sigma_{\text{MW}}^2 + \sigma_{\text{IGM}}^2 + \left(\frac{\sigma_{\text{host},0}}{1+z} \right)^2 + \delta^2 , \quad (3.1)$$

where σ_{MW} is the average galactic uncertainty and assumed to be 30 pc/cm^3 [69], δ is the DM fluctuations related to the spatial variation in cosmic electron density along the line-of-sight. As long as such fluctuations are not well-constrained by observations, we will treat them as a fixed value, $\delta = 230\sqrt{z} \text{ pc/cm}^3$ [18, 20]. The uncertainty of $DM_{\text{host},0}$ can be assumed as $\sigma_{\text{host},0} = 30 \text{ pc/cm}^3$ [70]. Finally, the uncertainty of IGM contribution (σ_{IGM}) can be calculated from error propagation of Eqs. 3.7 and 3.8 given by

¹<https://blinkverse.alkaidos.cn>

$$\sigma_{\text{IGM}} = Af_{\text{IGM},0} \left[\frac{\sigma_{D_L}^2}{c^2} + \frac{\sigma_{\text{I}}^2}{c^2} \right]^{1/2}, \quad (3.2)$$

where σ_{D_L} is the luminosity distance uncertainty that is calculated from the SNe, σ_{I} is the uncertainty of the quantity in Eq. 3.9.

3.1.2 BAO

For BAO dataset we use the results from DESI DR2 [5] that contains measurements from more than 14 million galaxies and quasars and are expressed in terms of three distances: the three-dimensional BAO mode (D_V/r_d), the radial mode (D_H/r_d) and the transverse mode (D_M/r_d). In the present work, we only consider the transverse mode due to its relation with the luminosity distance. From BAO scale measurements in the transverse direction at redshift z , the transverse comoving distance can be written assuming a flat Universe as

$$D_M(z) = c \int_0^z \frac{dz'}{H(z')}, \quad (3.3)$$

where it can be related to the luminosity distance from the below expression

$$D_L(z) = (1+z)D_M(z). \quad (3.4)$$

3.1.3 SNe Ia

Regarding SNe Ia observations, we use two different catalogs: Pantheon+ [71] (the complete catalog is available in the GitHub repository²), which contains the analysis of 1701 light curves of 1550 distinct SNe within the redshift range $0.001 < z < 2.3$.; and DES Y5 [72] (for the complete catalog, see the GitHub repository³), which comprises 1635 events, spanning a redshift range $0.02 < z < 1.13$, along with 194 high-quality external supernovae at redshifts below 0.1, for a total of 1829 supernovae. In the case of DES Y5 dataset, we remove the SNe with larger uncertainty ($\sigma_{\mu} > 2$ mag), and the remaining sample contains 1757 SNe.

From SNe dataset, we can obtain D_L by the distance moduli ($\mu(z)$) relation,

$$\mu(z) = m_B - M_B = 5 \log_{10} \left[\frac{D_L(z)}{1 \text{Mpc}} \right] + 25, \quad (3.5)$$

where m_B is the apparent magnitude and M_B is absolute magnitude, which here we fix consistent to H_0 from SH0ES collaboration [73], $M_B = -19.253 \pm 0.027$ mag.

The luminosity distance uncertainty relation can be expressed as:

$$\sigma_{D_L} = \frac{\ln 10}{5} D_L \cdot \sqrt{\sigma_{m_B}^2 + \sigma_{M_B}^2}, \quad (3.6)$$

being σ_{m_B} and σ_{M_B} the apparent and absolute magnitude uncertainties, respectively.

²<https://github.com/PantheonPlusSH0ES/DataRelease>

³<https://github.com/des-science/DES-SN5YR>

3.2 Methodology

In Reference [18], we proposed a cosmological model-independent approach, which we solve DM_{IGM} integral by parts, rewriting the $H(z)$ in terms of luminosity distance (D_L)⁴ assuming two parameterizations for the baryon fraction: time-dependent and constant cases. In the present paper, we consider the same approach, for which Eq. 2.3 can be written for the time-dependent case, $f_{\text{IGM}}(z) = f_{\text{IGM},0} + \alpha \frac{z}{1+z}$, as

$$DM_{\text{IGM}}(z) = A \left[\left(f_{\text{IGM},0} + \alpha \frac{z}{1+z} \right) \frac{D_L(z)}{c} - (f_{\text{IGM},0} + \alpha) \int_0^z \frac{D_L(z')}{(1+z')c} dz' \right], \quad (3.7)$$

where α is parameter that quantifies a possible evolution of f_{IGM} . In our analysis, both are free parameters and since f_{IGM} is understood to be an increasing function of the redshift, α assumes only positive values ($\alpha \geq 0$).

In the constant case ($f_{\text{IGM}}(z) = f_{\text{IGM},0}$), Eq. 2.3 can be written as

$$DM_{\text{IGM}}(z) = A f_{\text{IGM},0} \left[\frac{D_L(z)}{c} - \int_0^z \frac{D_L(z')}{(1+z')c} dz' \right]. \quad (3.8)$$

The second term in both expressions above can be numerically solved as (see [74]):

$$\int_0^z \frac{D_L(z')}{(1+z')} dz' = \frac{1}{2} \sum_{i=1}^N (z_{i+1} - z_i) \times \left[\frac{D_L(z_{i+1})}{(1+z_{i+1})} + \frac{D_L(z_i)}{(1+z_i)} \right].$$

From the above expressions, one can constrain the baryon fraction in the IGM by modeling the terms in $DM_{\text{ext}}^{\text{th}}$ quantity (Eq. 2.5) and comparing these theoretical predictions with the observed values of DM_{ext} . By combining well-localized FRBs with SNe and BAO (using Eq. 3.4 for the last one) datasets, we can obtain constraints on f_{IGM} and $DM_{\text{host},0}$ in a cosmology model-independent mode from the observational data sets described previously.

In order to estimate D_L , D_M and its uncertainty at the same redshift of FRBs, we perform a Gaussian Process (GP) reconstruction of the Pantheon+, DES Y5, and DESI DR2 datasets, respectively, using GaPP python library⁵. We perform a Monte Carlo Markov Chain (MCMC) analysis using the *emcee* package [76] to constrain the free parameters in our analysis: $f_{\text{IGM},0}$ and $DM_{\text{host},0}$ (for Constant case), and $f_{\text{IGM},0}$, α and $DM_{\text{host},0}$ (for Time-dependent case).

Since we are interested in a model-independent approach and to be consistent with our choice of M_B , we adopt the value for the Hubble constant in Eqs. 3.7 and 3.8 from SH0ES collaboration, $H_0 = 73.04 \pm 1.01$ km/s/Mpc [73]. We also assume model-independent values for the the sound horizon at the drag epoch, $r_d = 101 \pm 2.3 h^{-1}$ Mpc [77], to reconstruct D_M and for the baryon density parameter, $\Omega_b h^2 = 0.02235 \pm 0.00037$, from Big Bang Nucleosynthesis (BBN) analysis reported by [78].

4 Results

Figure 1 shows the posterior probability density function and $1-2\sigma$ contours for combinations of the free parameters $f_{\text{IGM},0}$, α and $DM_{\text{host},0}$ considering parameterizations constant (left

⁴The same method can be done, but instead of luminosity distance definition one can use the transverse comoving distance (D_M) from Eq. 3.4.

⁵For details of GaPP (<https://github.com/astrobangaly/GaPP>), see [75].

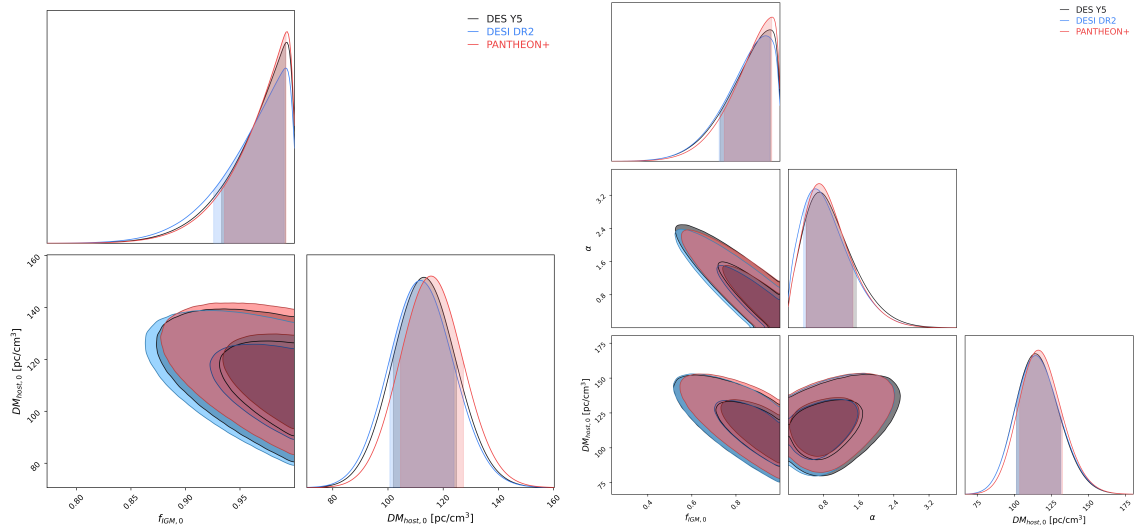


Figure 1. Constraints on the baryon fraction f_{IGM} parameters and the mean host galaxy contribution of dispersion measure $\text{DM}_{\text{host},0}$ for the three data combination. *Left:* considering the constant case. *Right:* for the time-dependent parameterization.

Table 1. Estimates of the f_{IGM} parameters and $\text{DM}_{\text{host},0}$.

Dataset	$f_{\text{IGM},0}$	α	$\text{DM}_{\text{host},0}$ [pc/cm^3]
Constant case			
FRB + DES Y5	$0.999^{+0.008}_{-0.066}$	-	113^{+12}_{-11}
FRB + DESI DR2	$0.999^{+0.010}_{-0.073}$	-	112^{+12}_{-11}
FRB + Pantheon+	$0.999^{+0.007}_{-0.066}$	-	116^{+12}_{-11}
Time-dependent case			
FRB + DES Y5	$0.955^{+0.003}_{-0.227}$	$0.70^{+0.84}_{-0.30}$	114^{+17}_{-13}
FRB + DESI DR2	$0.935^{+0.020}_{-0.211}$	$0.61^{+0.85}_{-0.26}$	114^{+18}_{-13}
FRB + Pantheon+	$0.972^{+0.009}_{-0.225}$	$0.71^{+0.76}_{-0.31}$	116^{+16}_{-12}

Panel) and time-dependent (right Panel). In Table 1 we present the results of the free parameters for both cases, considering the different datasets. For the constant case, the best-fit for the baryon fraction and host galaxy contribution is almost the same for the three datasets ($f_{\text{IGM},0} \sim 0.99^{+0.01}_{-0.07}$ and $\text{DM}_{\text{host},0} \sim 113 \pm 12 \text{ pc}/\text{cm}^3$ at 1σ level). For the time-dependent case, we estimate $f_{\text{IGM},0}$ ranging from $0.935^{+0.020}_{-0.211}$ (FRB + DESI DR2) to $0.972^{+0.009}_{-0.225}$ (FRB + Pantheon+) and from $0.61^{+0.85}_{-0.26}$ (FRB + DESI DR2) to $0.71^{+0.76}_{-0.31}$ (FRB + Pantheon+) for α at 1σ . While the host galaxy contribution we estimated ranged from $114^{+17}_{-13} \text{ pc}/\text{cm}^3$ (FRB + DES Y5) to $116^{+16}_{-12} \text{ pc}/\text{cm}^3$ (FRB + Pantheon+) (1σ). For both constant and time-dependent cases, the constraints on $f_{\text{IGM},0}$ and $\text{DM}_{\text{host},0}$ are compatible in 2σ level.

Comparing the results for the constant case with those obtained by Ref. [18], the values only agree at 2σ level for the cases where the fluctuation is $\delta = 50$ and $100 \text{ pc}/\text{cm}^3$ in Ref. [18], which is expected since here we are assuming $\delta = 230\sqrt{z} \text{ pc}/\text{cm}^3$. Now, considering the time-dependent case, in Ref. [18] we obtained for $f_{\text{IGM},0}$ varies from $f_{\text{IGM},0} = 0.483 \pm 0.066$

($\delta = 0 \text{ pc/cm}^3$) to $f_{\text{IGM},0} = 0.40 \pm 0.26$ ($\delta = 100 \text{ pc/cm}^3$), from $\alpha = 1.21 \pm 0.28$ ($\delta = 0 \text{ pc/cm}^3$) to $\alpha = 1.56 \pm 1.08$ ($\delta = 100 \text{ pc/cm}^3$) and from $\text{DM}_{\text{host},0} = 190.1 \pm 9.1 \text{ pc/cm}^3$ ($\delta = 0 \text{ pc/cm}^3$) to $\text{DM}_{\text{host},0} = 196.56 \pm 53.62 \text{ pc/cm}^3$ ($\delta = 100 \text{ pc/cm}^3$) at 1σ level. Comparing these values with the results estimated in the present paper, we can note that the results are not consistent at 2σ since the present value for $f_{\text{IGM},0}$ increased, being now in agreement with the values for the constant case (Tab. 1) and with other studies that used the same parameterization (see e.g. [79, 80] at 2σ level. While here we estimate values of the parameter α lower than the values we obtained in Ref. [18], agreeing with the values in Ref. [79, 80] (2σ). Note that the errors on the $f_{\text{IGM},0}$, α , and $\text{DM}_{\text{host},0}$ parameters depend on the number of points. Even with a value for DM fluctuations higher than the values assumed in Ref. [18], our results present uncertainties smaller than those in Ref. [18], which uses a sample with 17 events. Therefore, these results show that larger samples can improve the constraints (see [19] for a discussion about fluctuations and larger samples of FRBs).

Finally, it is worth mentioning that although DES, DESI, and Pantheon datasets point out a discrepancy in the estimate of the cosmological parameters, especially those of dark energy, here the constraints of the f_{IGM} are in concordance for these datasets. These results show the power of our method and the data.

Table 2. Estimates of the evidence and Bayes' factor.

Dataset	$\ln \mathcal{E}_i$	$\ln B_{ij}$
Constant case		
FRB + DES Y5	-96.181 ± 0.002	-
FRB + DESI DR2	-95.183 ± 0.002	-
FRB + Pantheon	-95.705 ± 0.002	-
Time-dependent case		
FRB + DES Y5	-96.712 ± 0.003	-0.531 ± 0.004
FRB + DESI DR2	-95.896 ± 0.002	-0.713 ± 0.003
FRB + Pantheon	-95.366 ± 0.002	$+0.339 \pm 0.003$

One interesting method to evaluate the performance of these two models studied and compare which of them the data prefers is the Bayesian model comparison, more precisely, from the Bayes' factor calculation. Such analysis can assess if the extra complexity of a given model or parameterization (here represented by the parameter α present in the time-dependent case) is required by the data, preferring the model that describes the data well over a large fraction of their prior volume (see e.g. [81, 82] for a detailed discussion). The Bayes' factor B_{ij} can be calculated from relation

$$B_{ij} = \frac{\mathcal{E}_i}{\mathcal{E}_j}, \quad (4.1)$$

defining the evidence as the marginal likelihood of the models, \mathcal{E}_i and \mathcal{E}_j correspond to the evidence of parameterizations \mathcal{P}_i and \mathcal{P}_j , respectively. The Jeffreys' scale [83] can be adopted to interpret the values of $\ln B_{ij}$ for the reference parameterization \mathcal{P}_j , where $\ln B_{ij} = 0 - 1$, $\ln B_{ij} = 1 - 2.5$, $\ln B_{ij} = 2.5 - 5$, and $\ln B_{ij} > 5$ indicate, respectively, an inconclusive, weak, moderate and strong preference of the parameterization \mathcal{P}_i with respect to \mathcal{P}_j . While negative values of $\ln B_{ij}$ mean preference in favour of \mathcal{P}_j .

Using the MultiNest algorithm [84–86] to compute the Bayesian evidence ($\ln \mathcal{E}$) and adopting the constant case as reference, we calculate the Bayes’ factor. In Table 2, we present the evidence and the Bayes’ factor ($\ln B_{ij}$) for each dataset. Since our results for the Bayes’ factor are negative for FRB + DES Y5 and FRB + DESI DR2 datasets, they indicate weak evidence in favor of constant parameterization. For FRB + Pantheon+, the result indicates weak evidence in favor of the time-dependent case. Therefore, these results show that a conclusive answer about the time evolution of f_{IGM} cannot be achieved from the current FRB observational data.

5 Conclusions and discussions

The latest BAO observation from DESI DR2 reports a possible tension in the Λ CDM model, indicating dynamical dark energy over a cosmological constant. This result motivates the exploration of alternative combinations of independent datasets to estimate the cosmological parameters.

In our previous work [18], we present a cosmological-model independent method, where we write $\text{DM}_{\text{IGM}}(z)$ expression in terms of $d_L(z)$, to constrain the f_{IGM} . We combined 17 FRBs with SNe from the Pantheon catalog and assumed two behaviors for f_{IGM} : the constant and time-dependent parameterizations. In the present paper, we revisited this paper, expanding the dataset by combining 107 well-localized FRBs with SNe measurements from Pantheon+ and DES Y5 and BAO data from DESI DR2.

We estimate $f_{\text{IGM},0} \sim 0.99_{-0.07}^{+0.01}$ (1σ level) for the constant case and $f_{\text{IGM},0}$ ranging from $0.935_{-0.211}^{+0.020}$ (FRB + DESI DR2) to $0.972_{-0.225}^{+0.009}$ (FRB + Pantheon+) at 1σ for time-dependent case. These results are consistent with our previous paper [18] (except for the time-dependent case where $\delta = 0$ and $10 \text{ pc}/\text{cm}^3$) and other works in the literature that used the same parameterization [79, 80]. To evaluate the performance of these two models, we also performed a Bayesian model comparison. The results showed weak evidence in favor of constant parameterization (FRB + DES and FRB + DESI DR2) and weak evidence⁶ in favor of the time-dependent case (FRB + Pantheon+).

Finally, we can note that the results indicate a concordance for the datasets used, even though they estimate cosmological parameters in disagreement, showing the robustness of our method. Also, the results present an improvement compared to the previous work, which could be attributed to the significantly different sample sizes used in these studies, reinforcing the interest in searching for a larger sample of FRBs.

Acknowledgements

TL thanks the financial support from the Conselho Nacional de Desenvolvimento Científico e Tecnológico (CNPq). This work was developed thanks to the High-Performance Computing Center at the National Observatory (CPDON).

⁶We also performed the analysis adopting H_0 from the Planck collaboration [87], $H_0 = 67.36 \pm 0.54$, along with a value of MB M_B consistent with this H_0 . The posterior distributions of the parameters remain similar, and the resulting Bayes factor continues to indicate only weak evidence in favor of the constant case across all datasets.

References

- [1] DESI Collaboration: A. Aghamousa, J. Aguilar, S. Ahlen, et al., *The DESI Experiment Part I: Science, Targeting, and Survey Design* (Dec., 2016), [arXiv:1611.00036].
- [2] M. Chevallier and D. Polarski, *Accelerating universes with scaling dark matter*, *Int. J. Mod. Phys. D* **10** (2001), 213-224, [arXiv:gr-qc/0009008 [gr-qc]].
- [3] E. V. Linder, *Exploring the expansion history of the universe*, *Phys. Rev. Lett.* **90** (2003), 091301 [arXiv:astro-ph/0208512 [astro-ph]].
- [4] E. M. Barboza, Jr. and J. S. Alcaniz, *A parametric model for dark energy* *Phys. Lett. B* **666** (2008), 415-419, [arXiv:0805.1713 [astro-ph]].
- [5] DESI Collaboration: M. Abdul-Karim, J. Aguilar, S. Ahlen, et al., *DESI DR2 Results II: Measurements of Baryon Acoustic Oscillations and Cosmological Constraints* (Mar., 2025), [arXiv:2503.14738].
- [6] E. Petroff, J. W. T. Hessels and D. R. Lorimer, *Fast radio bursts at the dawn of the 2020s*, *Astron. Astrophys. Rev.* **30** (March 2022) 2, [arXiv:2107.10113].
- [7] D. Thornton, B. Stappers, M. Bailes, et al., *A Population of Fast Radio Bursts at Cosmological Distances*, *Science* **341** (July, 2013) 53–56, [arXiv:1307.1628].
- [8] E. Petroff, M. Bailes, E. D. Barr, et al., *A real-time fast radio burst: polarization detection and multiwavelength follow-up*, *Mon. Not. Roy. Astron. Soc.* **447** (Feb., 2015) 246–255, [arXiv:1412.0342].
- [9] E. Petroff, E. D. Barr, A. Jameson, et al., *FRBCAT: The Fast Radio Burst Catalogue*, *Publications of the Astronomical Society of Australia* **33** (Sept., 2016) 7, [arXiv:1601.0354].
- [10] Platts E., Weltman A., Walters A., Tendulkar S. P., Gordin J. E. B., Kandhai S., *A living theory catalogue for fast radio bursts*, *Phys. Rep.* August, 2019 821, 1, [arXiv:1810.05836].
- [11] D. R. Lorimer, M. Bailes, M. A. McLaughlin, et al., *A Bright Millisecond Radio Burst of Extragalactic Origin*, *Science* 318 (Nov., 2007) **777**, [arXiv:0709.4301].
- [12] K. Dolag, B. M. Gaensler, A. M. Beck, et al., *Constraints on the distribution and energetics of fast radio bursts using cosmological hydrodynamic simulations*, *Mon. Not. Roy. Astron. Soc.* **451** (Jun., 2015) 4277–4289, [arXiv:1412.4829].
- [13] A. Walters, A. Weltman, B. M. Gaensler, et al., *Future Cosmological Constraints From Fast Radio Bursts*, *ApJ* **856** (Mar., 2018) 65, [arXiv:1711.11277].
- [14] J.-J. Wei, X.-F. Wu, H. Gao, *Cosmology with Gravitational Wave/Fast Radio Burst Associations*, *Astrophys. J. Lett.* **860** (Jun., 2018) L7, [arXiv:1805.12265].
- [15] H.-N. Lin, Y. Sang, *Probing the anisotropic distribution of baryon matter in the Universe using fast radio bursts*, *Chinese Phys. C* **45** (Dec., 2021) 125101, [arXiv:2111.12934].
- [16] Q. Wu, G. Q. Zhang, F. Y. Wang, *An 8% Determination of the Hubble Constant from localized Fast Radio Bursts*, *MNRAS Letters* **515** (Mar., 2022) L1–L5, [arXiv:2108.00581].
- [17] R. Reischke, S. Hagstotz, *Consistent Constraints on the Equivalence Principle from localised Fast Radio Bursts* (Feb., 2023), [arXiv:2302.10072].
- [18] T. Lemos, R. S. Gonçalves, J. C. Carvalho and J. S. Alcaniz, *Cosmological model-independent constraints on the baryon fraction in the IGM from fast radio bursts and supernovae data*, *EPJC* **83** (Feb., 2023) 138, [arXiv:2205.07926v2].
- [19] T. Lemos, R. S. Gonçalves, J. C. Carvalho and J. S. Alcaniz, *Forecasting constraints on the baryon mass fraction in the IGM from fast radio bursts and type Ia supernovae*, *EPJC* **83** (Dec., 2023) 1128, [arXiv:2307.06911v1].

- [20] R. Takahashi, K. Ioka, A. Mori, et al., *Statistical modelling of the cosmological dispersion measure*, *MNRAS* **502** (Jan., 2021) 2615–2629, [arXiv:2010.01560].
- [21] J. M. Shull, B. D. Smith, C. W. Danforth, *The Baryon Census in a Multiphase Intergalactic Medium: 30% of the Baryons May Still be Missing*, *ApJ* **759** (Nov., 2012) 23, [arXiv:1112.2706].
- [22] A. A. Meiksin, *The Physics of the Intergalactic Medium*, *Rev. Mod. Phys.* **81** (Oct., 2009) 1405–1469, [arXiv:0711.3358].
- [23] W. Deng, B. Zhang, *Cosmological Implications of Fast Radio Burst/Gamma-Ray Burst Associations*, *ApJ* **783** (Mar., 2014) L35, [arXiv:1401.0059].
- [24] H. Gao, Z. Li, and B. Zhang, *Fast Radio Burst/Gamma-Ray Burst Cosmography*, *ApJ* **788** (June, 2014) 189, [arXiv:1402.2498].
- [25] J.H. Taylor, and J.M. Cordes, *Pulsar Distances and the Galactic Distribution of Free Electrons*, *ApJ* **411** (Jul., 1993) 674–684.
- [26] J. M. Cordes, T. J. W. Lazio, *NE2001.I. A New Model for the Galactic Distribution of Free Electrons and its Fluctuations*, (Jul., 2002), [arXiv:astro-ph/0207156].
- [27] J. M. Yao, R. N. Manchester, and N. Wang, *A New Electron Density Model for Estimation of Pulsar and FRB Distances*, *ApJ* **835** (Jan., 2017) 29, [arXiv:1610.09448].
- [28] J.-P. Macquart, J.X. Prochaska, M. McQuinn, et al., *A census of baryons in the Universe from localized fast radio bursts*, *Nature* **581** (May, 2020) 391–395, [arXiv:2005.13161].
- [29] J. Xu, J. L. Han, *Extragalactic dispersion measures of fast radio bursts*, *Research in Astronomy and Astrophysics* **15** (Oct., 2015) 1629–1638, [arXiv:1504.00200].
- [30] K. Ioka, *The Cosmic Dispersion Measure from Gamma-Ray Burst Afterglows: Probing the Reionization History and the Burst Environment*, *Astrophys. J. Lett.* **598** (Dec., 2003) L79–L82, [astro-ph/0309200].
- [31] G. D. Becker, J. S. Bolton, M. G. Haehnelt, et al., *Detection of Extended He II Reionization in the Temperature Evolution of the Intergalactic Medium*, *MNRAS* **410** (Nov. 2010) 1096–1112, [arXiv:1008.2622].
- [32] J. Xu, Y. Feng, D. Li, *Blinkverse: A Database of Fast Radio Bursts*, *Universe* **9** (Jul., 2023) 330, [arXiv:2308.00336].
- [33] E. K. Mahony, R. D. Ekers, J.-P. Macquart, et al., *A search for the host galaxy of FRB171020*, *ApJL* **867** (Oct., 2018) L10, [arXiv:1810.04354].
- [34] M. Bhardwaj, A. Yu. Kirichenko, D. Michilli, et al., *A Local Universe Host for the Repeating Fast Radio Burst FRB 20181030A*, *ApJ* **919** (Sep., 2021) L24, [arXiv:2108.12122].
- [35] R. M. Shannon, K. W. Bannister, A. Bera, et al., *The Commensal Real-time ASKAP Fast Transient incoherent-sum survey*, *Publications of the Astronomical Society of Australia* (Jan., 2025) 1–36, [arXiv:2408.02083].
- [36] S.K. Ocker, J.M. Cordes, S. Chatterjee, et al., *The Large Dispersion and Scattering of FRB 20190520B Are Dominated by the Host Galaxy*, *ApJ* **931** (May, 2022) 87, [arXiv:2202.13458].
- [37] C. J. Law, B. J. Butler, J. X. Prochaska, et al., *A Distant Fast Radio Burst Associated with Its Host Galaxy by the Very Large Array*, *ApJ* **899** (Aug., 2020) 161, [arXiv:2007.02155].
- [38] M. Bhardwaj, B. M. Gaensler, V. M. Kaspi, et al., *A nearby repeating fast radio burst in the direction of M81*, *ApJ* **910** (Mar., 2021) L18, [arXiv:2103.01295].
- [39] L. N. Driessen, E. Barr, D. Buckley, et al., *FRB 20210405I: a nearby Fast Radio Burst localized to sub-arcsecond precision with MeerKAT*, *MNRAS* **527** (Jan., 2024) 3659–3673, [arXiv:2302.09787].

- [40] C. J. Law, K. Sharma, V. Ravi, et al., *Deep Synoptic Array Science: First FRB and Host Galaxy Catalog*, *ApJ* **967** (May, 2024) 18, [arXiv:2307.03344].
- [41] D. H. Gao, Q. Wu, J. P. Hu, et al., *Measuring Hubble constant using localized and unlocalized fast radio bursts* (2024), [arXiv:2410.03994].
- [42] L. Connor, V. Ravi, K. Sharma, et al., *A gas rich cosmic web revealed by partitioning the missing baryons* (2024), [arXiv:2409.16952].
- [43] CHIME/FRB Collaboration: M. Amiri, D. Amouyal, B. C. Andersen, et al., *A Catalog of Local Universe Fast Radio Bursts from CHIME/FRB and the KKO Outrigger* (2025), [arXiv:2502.11217].
- [44] S. Chatterjee, C. J. Law, R. S. Wharton, et al., *A direct localization of a fast radio burst and its host*, *Nature* **541** (Jan., 2017) 58–61, [arXiv:1701.01098].
- [45] S. Bhandari, K. E. Heintz, K. Aggarwal, et al., *Characterizing the FRB host galaxy population and its connection to transients in the local and extragalactic Universe*, *ApJ* **163** (Jan., 2022) 69, [arXiv:2108.01282].
- [46] D. Michilli, M. Bhardwaj, C. Brar, et al. *Sub-arcminute localization of 13 repeating fast radio bursts detected by CHIME/FRB*, *ApJ* **950** (Jun., 2023) 134, [arXiv:2212.11941].
- [47] B. Marcote, K. Nimmo, J. W. T. Hessels, et al., *A repeating fast radio burst source localised to a nearby spiral galaxy*, *Nature* **577** (Jan., 2020) 190–194, [arXiv:2001.02222].
- [48] K. W. Bannister, A. T. Deller, C. Phillips, et al., *A single fast radio burst localized to a massive galaxy at cosmological distance*, *Science*, **365** (June, 2019) 565–570, [arXiv:1906.11476].
- [49] J. X. Prochaska, J.-P. Macquart, M. McQuinn, et al., *The low density and magnetization of a massive galaxy halo exposed by a fast radio burst*, *Science* **366** (Oct., 2019) 231–234, [arXiv:1909.11681].
- [50] M. Bhardwaj, D. Michilli, Ai. Y. Kirichenko, et al., *Host Galaxies for Four Nearby CHIME/FRB Sources and the Local Universe FRB Host Galaxy Population* (2023), [arXiv:2310.10018].
- [51] S. Bhandari, E. M. Sadler, J. X. Prochaska, et al., *The host galaxies and progenitors of Fast Radio Bursts localized with the Australian Square Kilometre Array Pathfinder*, *ApJL* **895** (Jun., 2020) L37, [arXiv:2005.13160].
- [52] The CHIME/FRB Collaboration: B. C. Andersen, K. Bandura, M. Bhardwaj, et al., *CHIME/FRB Discovery of 25 Repeating Fast Radio Burst Sources*, *ApJ* **947** (Apr., 2023) 83, [arXiv:2301.08762].
- [53] V. Ravi, M. Catha, L. D’Addario, et al., *A fast radio burst localised to a massive galaxy*, *Nature*, **572** (July, 2019) 352–354, [arXiv:1907.0154].
- [54] K. E. Heintz, J. X. Prochaska, S. I. Simha, et al., *Host Galaxy Properties and Offset Distributions of Fast Radio Bursts: Implications for their Progenitors*, *ApJ* **903** (Nov., 2020) 152, [arXiv:2009.10747].
- [55] J. S. Chittidi, S. Simha, A. Mannings, et al., *Dissecting the Local Environment of FRB 190608 in the Spiral Arm of its Host Galaxy*, *ApJ* **922** (Nov., 2021) 173, [arXiv:2005.13158].
- [56] K. M. Rajwade, M. C. Bezuidenhout, M. Caleb, et al., *First discoveries and localisations of Fast Radio Bursts with MeerTRAP: a real-time, commensal MeerKAT survey*, *MNRAS* **514** (May, 2022) 1961–1974, [arXiv:2205.14600].
- [57] C. K. Day, S. Bhandari, A. T. Deller, et al., *ASKAP localisation of the FRB 20201124A source*, *The Astronomer’s Telegram* **14515** (Apr., 2021) 1.
- [58] S. Bhandari, A. C. Gordon, D. R. Scott, et al., *A non-repeating fast radio burst in a dwarf host galaxy*, *ApJ* (May, 2023) 67, [arXiv:2211.16790].

- [59] Shannon, R. M., *CRAFT Transient FRB Discovery Report for 2023-02-04, Transient Name Server Fast Radio Bursts* **287** (Feb., 2023) 1.
- [60] M. Caleb, L. N. Driessen, A. C. Gordon, et al., *A sub-arcsec localised fast radio burst with a significant host galaxy dispersion measure contribution*, *MNRAS* **524** (Jun., 2023) 2064–2077, [arXiv:2302.09754].
- [61] T. Cassanelli, C. Leung, P. Sanghavi, *A fast radio burst localized at detection to an edge-on galaxy using very-long-baseline interferometry*, *Nature Astronomy* **8** (Sep., 2024) 1429–1442, [arXiv:2307.09502].
- [62] J. Baptista, J. X. Prochaska, A. G. Mannings, et al., *Measuring the Variance of the Macquart Relation in Redshift–Extragalactic Dispersion Measure Modeling*, *ApJ* **965** (Apr., 2024) 57, [arXiv:2305.07022].
- [63] Ryder, S. D. and Bannister, K. W. and Bhandari, S. and et al., *A luminous fast radio burst that probes the Universe at redshift 1*, *Science* **382** (Oct., 2023) 294–299, [arXiv:2210.04680].
- [64] K. M. Rajwade, L. N. Driessen, E. D. Barr, et al., *A study of two FRBs with low polarization fractions localized with the MeerTRAP transient buffer system*, *MNRAS* **532** (Aug., 2024) 3881–3892, [arXiv:2407.02173].
- [65] V. Ravi, M. Catha, G. Chen, et al., *Deep Synoptic Array science I: discovery of the host galaxy of FRB 20220912A*, *ApJL* **949** (May, 2023) L3, [arXiv:2211.09049].
- [66] J. T. Faber, V. Ravi, S. K. Ocker, et al., *A Heavily Scattered Fast Radio Burst Is Viewed Through Multiple Galaxy Halos* (2024), [arXiv:2405.14182].
- [67] J. Tian, K. M. Rajwade, I. Pastor-Marazuela, et al., *Detection and localization of the highly active FRB 20240114A with MeerKAT*, *MNRAS* **533** (Sep., 2024) 3174–3193, [arXiv:2408.10988].
- [68] V. Shah, K. Shin, C. Leung, et al., *A Repeating Fast Radio Burst Source in the Outskirts of a Quiescent Galaxy*, *ApJL* **979** (Feb., 2025) L21, [arXiv:2410.23374].
- [69] R. N. Manchester, G. B. Hobbs, A. Teoh, et al., *The Australia Telescope National Facility Pulsar Catalogue*, *ApJ* **129** (Apr., 2005) 1993–2006, [astro-ph/0412641].
- [70] Z. Li, H. Gao, J.-J. Wei, et al., *Cosmology-independent Estimate of the Fraction of Baryon Mass in the IGM from Fast Radio Burst Observations*, *ApJ* **876** (May, 2019) 146, [arXiv:1904.0892].
- [71] D. Brout, D. Scolnic, B. Popovic, et al., *The Pantheon+ Analysis: Cosmological Constraints*, *ApJ* **938** (Oct., 2022) 110, [arXiv:2202.04077].
- [72] DES Collaboration: T. M. C. Abbott, M. Acevedo, M. Aguena, et al., *The Dark Energy Survey: Cosmology Results With 1500 New High-redshift Type Ia Supernovae Using The Full 5-year Dataset*, *ApJL* **973** (Oct., 2024) L14, [arXiv:2401.02929].
- [73] A. G. Riess, W. Yuan, L. M. Macri, et al., *A Comprehensive Measurement of the Local Value of the Hubble Constant with 1 km/s/Mpc Uncertainty from the Hubble Space Telescope and the SH0ES Team*, *ApJL* **934** (Jul., 2022) L7, [arXiv:2112.04510].
- [74] R. F. L. Holanda, J. C. Carvalho, and J. S. Alcaniz, *Model-independent constraints on the cosmic opacity*, *JCAP* **2013** (Apr., 2013) 027–027, [arXiv:1207.1694].
- [75] M. Seikel, C. Clarkson, M. Smith, *Reconstruction of dark energy and expansion dynamics using Gaussian processes*, *JCAP* **2012** (Jun., 2012) 036–036, [arXiv:1204.2832].
- [76] D. Foreman-Mackey, D. W. Hogg, D. Lang, et al., *emcee: The MCMC Hammer*, *Publications of the Astronomical Society of the Pacific* **125** (Mar., 2013) 306–312, [arXiv:1202.3665].
- [77] L. Verde, J. L. Bernal, A. F. Heavens, et al., *The length of the low-redshift standard ruler*, *MNRAS* **467** (May, 2017) 731–736, [arXiv:1607.05297].

- [78] R. Cooke, M. Pettini, C. C. Steidel, *One percent determination of the primordial deuterium abundance*, *ApJ* **855** (Mar., 2018) 102, [arXiv:1710.11129].
- [79] J.-J. Wei, Z. Li, H. Gao, and et al., *Constraining the Evolution of the Baryon Fraction in the IGM with FRB and $H(z)$ data*, *JCAP* **2019** (Sep., 2019) 039–039, [arXiv:1907.09772].
- [80] J.-P. Dai, and J.-Q. Xia, *Reconstruction of baryon fraction in intergalactic medium through dispersion measurements of fast radio bursts*, *MNRAS* **503** (Mar., 2021) 4576–4580, [arXiv:2103.08479v2].
- [81] R. Trotta, *Bayes in the sky: Bayesian inference and model selection in cosmology*, *Contemporary Physics* **49** (Mar., 2008) 71–104, [arXiv:0803.4089].
- [82] R. Trotta, *Bayesian Methods in Cosmology* (Jan., 2017), [arXiv:1701.01467].
- [83] H. Jeffreys, *Theory of Probability*, 3rd ed. (Oxford Univ. Press, Oxford, England, 1961).
- [84] F. Feroz, and M.P. Hobson, *Multimodal nested sampling: an efficient and robust alternative to MCMC methods for astronomical data analysis*, *MNRAS* **384** (Jan., 2008) 449–463, [arXiv:0704.3704].
- [85] F. Feroz, M.P. Hobson, and M. Bridges, *MultiNest: an efficient and robust Bayesian inference tool for cosmology and particle physics*, *MNRAS* **398** (Oct., 2009) 1601–1614, [arXiv:0809.3437].
- [86] F. Feroz, M. P. Hobson, E. Cameron, et al., *Importance Nested Sampling and the MultiNest Algorithm*, *The Open Journal of Astrophysics* **2** (Nov., 2019), [arXiv:1306.2144].
- [87] Planck Collaboration: N. Aghanim, Y. Akrami, M. Ashdown, et al., *Planck 2018 results. VI. Cosmological parameters*, *A&A* **641** (Sep., 2020) A6, [arXiv:1807.06209].

Table 3: Properties of FRBs

Name	z	DM _{ISM} [pc/cm ³]	DM _{obs} [pc/cm ³]	σ_{obs} [pc/cm ³]	Refs.
FRB 20121102A	0.19273	188.0	557.0	2.0	[44]
FRB 20180301A	0.3305	152.0	536.0	8.0	[45]
FRB 20180814	0.068	87.75	189.4	0.4	[46]
FRB 20180916B	0.0337	200.0	348.80	0.2	[47]
FRB 20180924B	0.3214	40.5	361.42	0.06	[48]
FRB 20181112A	0.4755	102.0	589.27	0.03	[49]
FRB 20181220A	0.2746	122.81	208.66	1.62	[50]
FRB 20181223C	0.03024	19.9	112.45	0.01	[50]
FRB 20190102C	0.2913	57.3	363.6	0.3	[51]
FRB 20190110C	0.12244	37	221.92	0.01	[52]
FRB 20190303A	0.064	29.39	222.4	0.7	[46]
FRB 20190418A	0.07132	70.2	182.78	1.62	[50]
FRB 20190425A	0.03122	49.25	127.78	1.62	[50]
FRB 20190523A	0.66	37.0	760.8	0.6	[53, 54]
FRB 20190608B	0.1178	37.2	338.7	0.5	[55]
FRB 20190611B	0.378	57.83	321.4	0.2	[54]
FRB 20190711A	0.522	56.4	593.1	0.4	[54]
FRB 20190714A	0.2365	38.0	504.13	2.0	[54]
FRB 20191001A	0.234	44.7	506.92	0.04	[54]
FRB 20191106C	0.10775	25	333.40	0.2	[52]
FRB 20191228A	0.2432	33.0	297.5	0.05	[45]
FRB 20200223B	0.06024	46	202.268	0.007	[52]
FRB 20200430A	0.16	27.0	380.25	0.5	[54]
FRB 20200906A	0.3688	36	577.8	0.02	[45]
FRB 20201123A	0.0507	251.93	433.55	0.0036	[56]
FRB 20201124A	0.098	123.2	413.52	0.5	[57]
FRB 20210117A	0.2145	34.4	730.0	1.0	[58]
FRB 20210320	0.2797	42.2	384.8	0.3	[59]
FRB 20210410D	0.1415	56.2	578.78	2.0	[60]
FRB 20210603A	0.1772	40.0	500.147	0.004	[61]
FRB 20210807D	0.12927	121.2	251.9	0.2	[35]
FRB 20211127I	0.0469	42.5	234.83	0.08	[35]
FRB 20211203C	0.3439	63.4	636.2	0.4	[62]
FRB 20211212A	0.0715	27.1	206.0	5.0	[35]
FRB 20220105A	0.2785	22.0	583	1.0	[62]
FRB 20220204A	0.4	50.7	612.2	0.05	[42]
FRB 20220207C	0.043040	79.3	262.38	0.01	[40]
FRB 20220208A	0.351	101.6	437	0.6	[42]
FRB 20220307B	0.248123	135.7	499.27	0.06	[40]
FRB 20220310F	0.477958	45.4	462.24	0.005	[40]
FRB 20220330D	0.3714	38.6	468.1	0.85	[42]
FRB 20220418A	0.622000	37.6	623.25	0.01	[40]
FRB 20220501C	0.381	31	449.5	0.2	[35]

Name	z	DM_{ISM} [pc/cm ³]	DM_{obs} [pc/cm ³]	σ_{obs} [pc/cm ³]	Refs.
FRB 20220506D	0.30039	89.1	396.97	0.02	[40]
FRB 20220509G	0.089400	55.2	269.53	0.02	[40]
FRB 20220610A	1.016	31.0	1458.15	0.2	[63]
FRB 20220717A	0.36295	118	637.34	3.52	[64]
FRB 20220725A	0.1926	31	290.4	0.3	[35]
FRB 20220726A	0.361	89.5	686.55	0.01	[42]
FRB 20220825A	0.241397	79.7	651.24	0.06	[40]
FRB 20220831A	0.262	1019.50	1146.25	0.2	[42]
FRB 20220912A	0.0771	125.00	219.46	0.042	[65]
FRB 20220914A	0.113900	55.2	631.28	0.04	[40]
FRB 20220918A	0.491	41	656.8	0.8	[35]
FRB 20220920A	0.158239	40.3	314.99	0.01	[40]
FRB 20221012A	0.284669	54.4	441.08	0.7	[40]
FRB 20221106A	0.2044	35	343.8	0.8	[35]
FRB 20221219A	0.554	44.4	706.7	0.6	[66]
FRB 20230526A	0.1570	50	361.4	0.2	[35]
FRB 20230708A	0.105	50	411.51	0.05	[35]
FRB 20230718A	0.035	396	477.0	0.5	[35]
FRB 20230814A	0.5535	104.9	696.35	0.5	[42]
FRB 20230902A	0.3619	34	440.1	0.1	[35]
FRB 20231226A	0.1569	145	329.9	0.1	[35]
FRB 20240114A	0.13	49.7	527.65	0.01	[67]
FRB 20240201A	0.042729	38	374.5	0.2	[35]
FRB 20240209A	0.1384	55.5	176.49	0.01	[68]
FRB 20240210A	0.023686	31	283.73	0.05	[35]
FRB 20240310A	0.1270	36	601.8	0.2	[35]